The Cloud Physics Lidar:

Instrument Description and Initial Measurement Results

Dr. Matthew McGill
NASA Goddard Space Flight Center
Code 912
Greenbelt, MD 20771
phone: 301-614-6281
fax: 301-614-5492
email: mcgill@virl.gsfc.nasa.gov

Mr. Dennis Hlavka
Science Systems and Applications, Inc.
NASA Goddard Space Flight Center
Code 912
Greenbelt, MD 20771
phone: 301-614-6278
fax: 301-614-5492
email: sgdlh@virl.gsfc.nasa.gov

Mr. William Hart
Science Systems and Applications, Inc.
NASA Goddard Space Flight Center
Code 912
Greenbelt, MD 20771
phone: 301-614-6272
fax: 301-614-5492
email: billhart@virl.gsfc.nasa.gov

Dr. James Spinhirne
NASA Goddard Space Flight Center
Code 912
Greenbelt, MD 20771
phone: 301-614-6274
fax: 301-614-5492
email: jspin@virl.gsfc.nasa.gov

Mr. V. Stanley Scott
NASA Goddard Space Flight Center
Code 912
Greenbelt, MD 20771
phone: 301-614-6280
fax: 301-614-5492
email: stan@virl.gsfc.nasa.gov

Abstract

The new Cloud Physics Lidar (CPL) has been built for use on the NASA ER-2 high altitude aircraft. The purpose of the CPL is to provide multi-wavelength measurements of cirrus, subvisual cirrus, and aerosols with high temporal and spatial resolution. The CPL utilizes state-of-the-art technology with a high repetition rate, low pulse energy laser and photon-counting detection. The first deployment for the CPL was the SAFARI-2000 field campaign during August-September 2000. We provide here an overview of the instrument and initial data results to illustrate the measurement capability of the CPL.

OCIS Codes: 010.1100, 010.3640, 280.0280, 280.3640

Introduction

The effect of clouds and aerosols on regional and global climate is of great importance. An important element of the NASA climate and radiation science program is field studies that incorporate airborne remote sensing and in situ measurements of clouds and aerosols. These field experiments involve coordination of ground based and satellite measurements with the airborne observations. The goals of such experiments include testing satellite remote sensing retrievals, developing advanced remote sensing techniques and providing fundamental advances in knowledge of cloud radiation and microphysical properties.

One of the most important components of airborne remote sensing experiments is the high altitude NASA ER-2 aircraft. Because the ER-2 typically flies at about 65,000 feet (20 km), its instruments are above 94% of the earth's atmosphere,

thereby allowing ER-2 instruments to function as spaceborne instrument simulators. The ER-2 provides a unique platform for atmospheric profiling, particularly for active remote sensing instruments such as lidar. A typical ER-2 remote sensing experiment combines multispectral passive cloud remote sensing with active lidar and/or radar profiling. Much of the science with the data is application and testing of cloud remote sensing between satellite measurements. In these situations, active lidar profiling is especially valuable because the cloud height structure, up to the limit of signal attenuation, is unambiguously measured.

The Cloud Lidar System (CLS) was the first high altitude lidar system designed specifically for studying clouds and aerosols[1-3] and was first flown on the ER-2 aircraft in 1983. In subsequent years, the CLS was modified as necessary to stay current with improving technology. The CLS participated in a large number of major field campaigns including TOGA-COARE, CEPEX, FIRE, and SUCCESS.[4-8] The CLS historically provided basic lidar cloud and aerosol observations at 1064 nm and 532 nm. Standard CLS data products included cloud height and cloud boundary, cloud and aerosol structure, and multiple layering up to the limit of signal attenuation.

The CLS data has been applied in studies involving retrieval of cloud radiation parameters. The visible optical thickness for transmissive clouds can, in principal, be obtained from the decrease in signals beyond the lower cloud boundary,[3] but both multiple scattering and practical limitations of the analog signal acquisition of the CLS introduce significant uncertainties. Such limitations eventually led investigators to consider a new version of CLS that would be designed to alleviate

the difficulties inherent in the CLS hardware. However, before science issues alone could determine a course of action, time caught up with the CLS and spare parts became a serious issue. A decision had to be made on replacing the original data system with newer components. That, coupled with increasing desires for enhanced science capabilities, strongly suggested a new instrument would be more cost effective in the long term. Ultimately, a decision was made to develop an entirely new instrument to replace the CLS. The new instrument would have increased science capabilities, smaller size, reduced mass, and would utilize newer component technologies.

The Cloud Physics Lidar (CPL)

In designing the Cloud Physics Lidar (CPL), three primary considerations drove the instrument design: (1) make the system eye-safe at the operating altitude; (2) make the system as lightweight as possible, yet rugged; and (3) use solid state photon-counting detectors. In addition, all mechanical and safety considerations relating to the ER-2 aircraft had to be accommodated.

In recent years there have been significant advances in the approach to lidar design. A now-proven approach is to use a high repetition rate laser, operating at multiple kHz rather than tens of Hz, but at low pulse energies. Ground based systems of this type, such as the MicroPulse Lidar,[9,10] have been in use since the early 1990's. Advantages of using a high repetition rate laser are the potential of eye safety from low pulse energies, more compact size, greater reliability, and turnkey ease of use. A basic requirement of using a high repetition rate laser is a narrow field of view, along with narrowband filtering, to minimize solar background

noise. An added advantage is that the field of view is small enough to essentially eliminate multiple scattered signal.

Because the pulse energy is low, the instrument can be designed to use photon-counting detection. Solid-state photon-counting detectors are readily available and have good quantum efficiencies with low thermal noise. More importantly, the photon-counting detectors permit easy data inversion without the need for complicated calibration schemes or calibration of log-amplifiers, as is needed when using analog detectors. The disadvantage of photon-counting detectors is their inherently small dynamic range. However, use of photon-counting detectors along with high repetition rate lasers still allows for wide dynamic range in the measured signal, the dynamic range being attained by accumulating over many pulses.

Science goals immediately dictated that the system be designed around a three wavelength laser. The laser transmitter is a solid-state, conductively cooled system made by LiteCyles, Inc. The laser is a neodymium vanadate (Nd:YVO$_4$) oscillator with doubling and tripling crystals generating 1064 nm, 532 nm, and 355 nm outputs simultaneously and collinear. The laser head is housed in the instrument box and is fiber optically coupled to the power supply and diodes. The pump diodes are located outside the instrument box to aid in dissipating the heat generated by the diodes and associated electronics. Output energies at each wavelength are given in Table 1.

As is done with the MicroPulse Lidars, the telescope is used as a beam expander. However, unlike the MicroPulse Lidars, the CPL utilizes an 8-inch diameter off-axis

parabola as the telescope primary. The off-axis parabola not only permits a rugged and robust design, but also eliminates most obscurations to both the outgoing and incoming beams. In fact, none of the outgoing light is lost to obscurations, and only about 20% of the receiver aperture is obscured. Return signal collected by the telescope is separated into wavelength components by use of dichroics. The 1064 nm return is further separated into parallel and perpendicular polarization components. Once the wavelengths are separated, each component is passed through a narrowband interference filter and fiber optically coupled to an appropriate detector. For the 532 and 1064 nm channels a pair of matched interference filters are used to provide better solar rejection. A half-wave plate is located in the 1064 nm path to allow calibration of the parallel and perpendicular channels. A simplified schematic diagram of the CPL optics is shown in Figure 1.

As mentioned previously, overall instrument design was driven by a desire to use simple photon-counting detectors. The 1064 nm detectors are EG&G single photon counting modules (SPCMs). These detectors have approximately 3% quantum efficiency and low thermal noise (less than 200 counts per second). The 532 nm channel also utilizes EG&G SPCMs, the quantum efficiency being approximately 60% at that wavelength. The 355 nm channel uses a Hamamatsu photomultiplier tube to allow for good quantum efficiency (~20%) and larger dynamic range for the enhanced Rayleigh signal. Outputs from the detectors are counted by a multichannel range-gating card made by ASRC Aerospace Corporation.

The laser head and transmit optics are mounted on one side of an optical breadboard. The receiver optics are mounted on the back side of the same

breadboard. The optical breadboard is housed in a sealed box to maintain a clean, thermally stable, and dry environment. For vibration isolation the breadboard mounts to the box via a three-point kinematic mounting system. Figure 2 shows front and back views of the optical breadboard with all components mounted. The breadboard is compact to fit within the ER-2 and measures only 22 x 12 inches.

Science capabilities of the Cloud Physics Lidar

The CPL provides a complete ensemble of cloud physics information. Primary data products include:

- Cloud profiling with 30 m vertical and 200 m horizontal resolution at 1064 nm, 532 nm, and 355 nm, providing cloud location and internal backscatter structure.

- Aerosol, boundary layer, and smoke plume profiling at all three wavelengths, providing calibrated profiles of backscatter coefficients.

- Depolarization ratio to determine the phase (e.g., ice or water) of clouds using the 1064 nm output.

- Cloud particle size determined from comparison of backscatter at the three wavelengths.

- Determination of optical depth for both cloud and aerosol layers (up to the limit of signal attenuation, ~optical depth 3).

- Direct determination of the optical depth of cirrus clouds (up to ~optical depth 3) using the 355 nm output.

- Determination of extinction-to-backscatter parameter.

The CPL provides information to permit a comprehensive analysis of radiative and optical properties of optically thin clouds. To determine the effects of particulate layers on the radiative budget of the earth-atmosphere system certain information about the details of the layer and its constituents is required. The effect of cirrus clouds on the earth's radiation budget has long been recognized.[11] The interaction of radiation with cirrus clouds, termed cloud radiative forcing, is important for both regional and global scale energy budgets. The information required to compute the radiative forcing includes the vertical distribution of short wave cross section, a parameter that the CPL can provide up to the limits of optical signal attenuation.

Using optical depth measurements determined from attenuation of Rayleigh and particulate scattering, and using the integrated backscatter, the extinction-to-backscatter parameter can be derived under favorable atmospheric conditions. This permits rapid analysis of cloud optical depth since only lidar data is required; there is no need to use other instrumentation. Using the derived extinction-to-backscatter ratio, the internal cloud extinction profile can then be obtained.

The CPL uses photon-counting detectors with a high repetition rate laser to maintain a large signal dynamic range. This dramatically reduces the time required to produce reliable and complete data sets. The goal of the CPL analysis is to provide data within 24 hours of a flight including: (1) cloud and aerosol quick-look pictures, (2) cloud and aerosol layer boundaries, and (3) depolarization information. The optical depth determinations require more careful analysis. Determination of optical depths for uncomplicated layers of cirrus clouds with homogeneous scattering characteristics can be completed within a day using an automated

analysis algorithm. However, situations where the cloud layering and structure is complex, which often precludes an automated data processing algorithm, may require several weeks for processing.

Multiply-scattered signal is a known problem for cloud and aerosol remote sensing by conventional lidar. For a standard lidar equation it is generally assumed that only first-order scattering is collected by the receiver. However, most lidar systems have wide receiver fields of view that necessarily collect multiply-scattered signal when a dense medium (e.g., cloud) is encountered. When multiply-scattered signal is present but not accounted for in data analysis, incorrect estimates of extinction-to-backscatter and optical depth can occur. Multiple scattering is difficult to predict due to the dependence on both the measurement geometry and particle size. The CLS receiver had a field of view of 1.6 mrad full angle. When dense media was encountered, the multiply-scattered contribution was significant. For CLS retrievals, the correction to direct optical thickness was approximately a factor of two but could vary by over 50%.[12] The new CPL receiver has a field of view of only 100 μrad full angle. While not entirely eliminating multiply scattered signals, the small field of view does greatly minimize collection of multiply scattered signals. Simulations show that the amount of multiple scattered signal should be 5% or less of the total measured signal for thin cirrus, and no more than 15% for clouds of optical depth 2.

First flights and sample data

The first field deployment for the CPL was the Southern African Regional Science Initiative (SAFARI) campaign in southern Africa during August-September

2000.[13,14] The purpose of SAFARI was to study the unique climatology of southern Africa, with particular emphasis on biomass burning and other regional emissions. During the SAFARI campaign, the CPL provided data on cloud height and structure as well as aerosol and smoke plume structure. The goal is to use CPL data to determine quantitative optical characteristics of both clouds and smoke layers. The CPL data will be used in conjunction with other airborne and ground-based instrumentation, as well as satellite data, to quantify and validate the regional emissions. Data from the SAFARI campaign will be used to understand the linkages between land-atmosphere processes. While detailed analysis of data will be the focus of future articles, we present here some initial results to demonstrate the data collection capability of the CPL.

As with any lidar, instrument corrections (e.g., overlap, detector deadtime) must be applied and the system must be calibrated before data products can be retrieved. For the CPL we have developed a standardized calibration routine. The most important part of the calibration is knowing how much energy is transmitted to the atmosphere for each measurement. To measure the output energy of the laser an energy monitor detector (a photodiode) samples the laser output. Separate detectors are used for each wavelength, thus ensuring that each wavelength can be independently and accurately calibrated. The energy monitor detector is calibrated to the laser energy in a laboratory setting. This calibration provides a relationship between laser energy and energy monitor output that is used to energy normalize the CPL measurements during operation. During operation the energy monitors sample the laser energy on every pulse to ensure an accurate measure of the output energy is obtained. To obtain the instrument calibration constant the measured,

energy normalized CPL profile is adjusted to match a molecular profile at high altitude. The molecular profile is obtained either through standard atmosphere models or, if available, balloon soundings or other local sources of temperature/pressure profiles. In the data processing stage, the instrument calibration is calculated for every profile and then averaged over five minute intervals.

During the SAFARI campaign the CPL instrument operated properly and good data from the 532 nm and 1064 nm channels were obtained. A custom optic for the 355 nm channel was not delivered in time which precluded use of that channel for the SAFARI mission. During the SAFARI mission 120 flight hours of data were obtained by CPL with no problems or failures. Figure 3 shows a plot of attenuated backscatter over the course of an entire flight on September 25, 2000. The top panel is the 1064 nm attenuated backscatter (sum of both parallel and perpendicular channels), and the middle panel is the 532 nm attenuated backscatter. The bottom panel in Figure 3 is the derived total particulate optical depth by wavelength. As evidenced in Figure 3, the signal to noise in the both the 1064 nm and 532 nm data is extremely good. At higher altitudes the 1064 profiles reflect the absence of both aerosol and molecular scatterers at high altitudes. The standard deviation of the total particulate optical depth, calculated by averaging over periods where clouds are not present and natural variability is minimal, varies from 0.04-0.08 for 532 nm and 0.02-0.03 for 1064 nm. To aid in interpreting the data, Figure 4 shows the flight tracks for all data segments used in this paper.

During the SAFARI campaign there was only one flight that encountered any significant cirrus clouds. A two hour segment of data from September 4, 2000 is shown in Figure 5. The top panel shows the 532 nm attenuated backscatter while the bottom panel shows the retrieved cirrus optical depth by wavelength. For this data segment the extinction-to-backscatter ratio (S-ratio) was pre-set to 29.5 sr for both the 532 nm and 1064 nm channels if the ratio could not be calculated. The retrieved cirrus optical depth exhibits no wavelength dependence. This result verifies proper behavior of the optical depth retrieval algorithm, because cirrus clouds are expected to be "white" scatterers (e.g, all wavelengths are scattered equally).

Of particular interest in the SAFARI campaign were optical properties of the planetary boundary layer due to smoke from extensive biomass burning. Figure 6 shows a two hour segment of data from September 1, 2000. The top panel is the 1064 nm total backscatter showing the structure of aerosols within the boundary layer. The boundary layer is capped by a strong inversion, with little aerosol above the capping level. The bottom panel in Figure 6 is the aerosol optical depth by wavelength for the boundary layer, calculated from the top of the layer down to the ground. Two features are evident in the data. First, the optical depth of the boundary layer increases as the flight proceeds. Second, there is a strong wavelength dependence presumably due to large concentrations of smoke particles. In fact, in the latter half of the data segment the optical depth becomes large enough that the 532 nm lidar signal is almost fully attenuated before reaching the ground, thereby resulting in noisy 532 nm retrievals. For processing this data segment the extinction-to-backscatter ratio (S-ratio) was fixed at 57 sr for the 532

nm and 49 sr for the 1064 nm. These S-ratio values are consistent with a smoke-polluted boundary layer.[15]

As part of the SAFARI field campaign, ground-based MicroPulse Lidar systems were deployed at two field locations. One system was located in the Skukuza National Park in South Africa, the other in Mongu, Zambia. At several times during the campaign the ER-2 was directed to overfly the MicroPulse Lidar sites to allow calibration and comparison of the ground-based and airborne sensors. Figure 7 shows one such comparison of extinction profiles derived from the CPL and MicroPulse Lidar on August 22, 2000. In this particular case, the ER-2 flew no closer than 5 miles to the MicroPulse Lidar site. This difference in exact location probably accounts for differences between the profiles in the lowest kilometer. In this example the CPL profile is a 30-second average while the MicroPulse Lidar profile is a 30-minute average. In calculating the extinction profiles, the extinction-to-backscatter ratio (S-ratio) for the 532 nm channel was fixed at 61 sr while the MicroPulse Lidar (operating at 523 nm) S-ratio was fixed at 74 sr. Both lidars used Aerosol Robotic Network (AERONET) CIMEL[16] optical depth measurements co-located at the MicroPulse Lidar site to calculate the S-ratios.

Also participating in the SAFARI campaign was the NASA Ames Airborne Tracking 14-Channel sunphotomer (AATS-14) onboard the University of Washington CV-580 aircraft. The AATS-14 measures atmospheric transmission (and hence optical depth and extinction) in bands from 354 nm out to 1558 nm.[17] The channels of interest to CPL are those at 525 nm and 1020 nm, close to the CPL wavelengths. The AATS-14 extinction profiles are overplotted in Figure 7. The agreement with

the CPL 1064 nm profile is quite good. At the shorter 532 nm wavelength the agreement is also good, although as expected there is greater wavelength dependence due to the differences in operating wavelength among the three instruments. Nonetheless, this result indicates that the CPL instrument and analysis algorithms do provide accurate measurements of aerosol optical properties.

Conclusion

During 1999-2000 a new cloud and aerosol lidar system, the Cloud Physics Lidar, was built for use on the high altitude NASA ER-2 aircraft. The CPL provides measurements at three wavelengths to permit a comprehensive study of cloud and aerosol properties. The CPL is designed around a high repetition rate, low pulse energy laser transmitter. Photon-counting detection is used to simplify the data inversion process. Although photon-counting detectors have limited bandwidth, use of the high repetition rate laser allows for large dynamic range through pulse accumulation at low pulse energy.

The first field deployment for the CPL was the SAFARI-2000 campaign during August-September 2000. During the SAFARI mission the CPL provided measurements of boudary layer structure and optical properties to aid in studies of biomass burning. Examples have been shown to illustrate the data collection capability of the CPL. It is demonstrated that aerosol variability and structure are measured during daylight conditions. Retrieved optical depth estimates are consistent with expectations. Comparisons of CPL-derived extinction profiles compare favorably with those from other lidar and in-situ instruments.

Acknowledgements

References

(1) Spinhirne, J.D., M.Z. Hansen, and L.O. Caudill, "Cloud top remote sensing by airborne lidar," *Applied Optics*, **21**, 1564-1571 (1982).

(2) Spinhirne J.D., M.Z. Hansen, and J. Simpson, "The structure and phase of cloud tops as observed by polarization lidar," *Journal of Applied Meteorology*, **22**, 1319 (1983).

(3) Spinhirne, J.D. and W.D. Hart, "Cirrus structure and radiative parameters from airborne lidar and spectral radiometer observations: the 28 October 1986 FIRE study," *Monthly Weather Review*, **118** 2329-2343 (1990).

(4) Spinhirne, J.D., W.D. Hart, and D.L. Hlavka, "Cirrus infrared parameters and shortwave reflectance relations from observations," *Journal of the Atmospheric Sciences*, **53**, 1438-1458 (1996).

(5) Duda, D.P, J.D. Spinhirne, and W.D. Hart, "Retrieval of contrail microphysical properties during SUCCESS by the split-window method," *Geophysical Research Letters*, **25**, 1149-1152 (1998).

(6) Spinhirne, J.D., W.D. Hart and D. Duda, "Evolution of the morphology and microphysics of contrail cirrus from airborne active and passive remote sensing," *Geophysical Research Letters*, **23**, 1153-1156 (1998).

(7) Wang, J.R., P. Racette, J.D. Spinhirne, K.F. Evans, and W.D. Hart, "Observations of cirrus clouds with airborne MIR, CLS, and MAS during SUCCESS," *Geophysical Research Letters*, **25**, 1145-1148 (1998).

(8) Heymsfield, A.J., G.M. McFarquhar, W.D. Collins, J.A. Goldstein, F.P.J. Valero, J. Spinhirne, W. Hart, and P. Pilewskie, "Cloud properties leading to highly reflective tropical cirrus: Interpretations from CEPEX, TOGA COARE, and Kwajalein, Marshall Islands," *Journal of Geophysical Research-Atmospheres*, **103**, 8805-8812 (1998).

(9) Spinhirne, J.D., "Micro Pulse Lidar," *IEEE Transactions on Geoscience and Remote Sensing*, **31**, 48-55 (1993).

(10) Spinhirne, J.D., J.A.R. Rall, and V.S. Scott, "Compact eye safe lidar systems," *The Review of Laser Engineering*, **23**, 112-118 (1995).

(11) Kaufman, Y.J., P.V. Hobbs, V.W.J.H Kirchoff, P. Artaxo, L.A. Remer, B.N. Holben, M.D. King, D.E. Ward, E.M. Prins, K.M. Longo, L.F. Mattos, C.A. Nobre, J.D. Spinhirne, Q. Ji, A.M. Thompson, J.F. Gleason, S.A. Christopher, and S.C. Tsay, "Smoke, Clouds, and Radiation – Brazil (SCAR-B) experiment," *Journal of Geophysical Research – Atmospheres*, **103**, 31783-31808 (1998).

(12) Platt, C. M. R., J. D. Spinhirne and W. D. Hart, "Optical and microphysical properties of a cold cirrus cloud: Evidence for regions of small ice particles," *Journal of Geophysical Research*, **94**, 11151, (1989).

(13) Swap R.J., and J. Privette, "Overview of the Southern African Regional Science Initiative – SAFARI 2000," IEEE 1999 International Geoscience and Remote Sensing Symposium, Hamburg Germany, 28 June – 2 July, 1999.

(14) Swap, B., J. Privette, M. King, D. Starr, T. Suttles, H. Annegarn, M. Scholes and C.O. Justice, "SAFARI 2000: a southern African regional science initiative," *EOS Earth Observer*, **10**(6), 25-28 (1998).

(15) Ackerman, J., "The extinction-to-backscatter ratio of tropospheric aerosol: A numerical study," *Journal of Atmospheric and Oceanic Technology*, 15, 1043-1050 (1998).

(16) Holben, B.N., T.F. Eck, I. Slutsker, D. Tanre, J.P. Buis, A. Setzer, E. Vermote, J.A. Reagan, Y.J. Kaufman, T. Nakajima, F. Lavenu, I. Jankowiak, and A. Smirnov, "AERONET - A federated instrument network and data archive for aerosol characterization," *Rem. Sens. Environ.*, **66**, 1-16 (1998).

(17) Schmid, B., J.M. Livingston, P.B. Russell, P.A. Durkee, H.H. Jonsson, D.R. Collins, R.C. Flagan, J.H. Seinfeld, S. Gasso, D.A. Hegg, E. Ostrom, K.J. Noone, E.J. Welton, K.J. Voss, H.R Gordon, P. Formenti, and M.O. Andreae, "Clear-sky studies of lower tropospheric aerosol and water vapor during ACE-2 using airborne sunphotomoeter, airborne in-situ, space-borne, and ground-based measurements," *Tellus B 52*, 568-593 (2000).

Table 1: CPL system parameters

PARAMETER	VALUE
Wavelengths	1064, 532, and 355 nm
Laser type	solid-state Nd:YVO$_4$
Laser repetition rate	5 kHz
Laser output energy	50 uJ at 1064 nm 25 uJ at 532 nm 50 uJ at 355 nm
Telescope diameter	8 inches
Telescope type	off-axis parabola
Telescope field of view	100 microradians, full angle
Effective filter bandwidth (full width, half-height)	240 pm at 1064 nm 120 pm at 532 nm 150 pm at 355 nm
Filter efficiency	81% at 1064 nm 60% at 532 nm 45% at 355 nm
Detector efficiency (all detectors fiber-coupled)	3% at 1064 nm 60% at 532 nm 10% at 355 nm
Raw data resolution	1/10 second (30 m vertical by 20 m horizontal)
Processed data resolution	1 second (30 m vertical by 200 m horizontal)

FIGURE CAPTIONS

Figure 1: Simplified optical diagram of CPL. Components are labeled as follows: F are interference filters, M are mirrors, and W is a half-wave plate. Components lying above the dashed line are mounted on one side of the optical breadboard, components lying below are mounted on the opposite side.

Figure 2: a) Photo of transmitter side of optical breadboard, showing the laser head and off-axis mirror. b) Photo of receiver side of optical breadboard, showing the component layout and the different wavelength channels.

Figure 3: CPL data from September 25, 2000. Top panel shows 1064 nm attenuated backscatter profiles. Middle panel is 532 nm attenuated backscatter profiles. Bottom panel is derived total optical depth. The green trace is the 532 nm optical depth, red trace is 1064 nm. Plot shows the entire flight, illustrating the variability and structure that can be seen in the lidar data. Dense clouds are bright white and cloud shadows are present whenever the lidar signal cannot penetrate through a layer.

Figure 4: ER-2 flight tracks for September 1, 4, and 25, 2000.

Figure 5: Cirrus optical depth from September 4, 2000. Plot shows two hours of data. Top panel is the 532 nm attenuated backscatter coefficient, bottom panel is the retrieved cirrus optical depth. The cirrus optical depth is the optical depth due to particulates over the region 9 km to 15 km. In the bottom panel, the green trace

is the 532 nm optical depth and the red trace is the 1064 nm optical depth. As expected, there is no wavelength dependence to the cirrus optical depth.

Figure 6: Planetary boundary layer (PBL) optical depth from September 1, 2000. Plot shows two hours of data. Top panel is the 1064 nm attenuated backscatter coefficient, bottom panel is the resultant aerosol optical depth for the PBL only. In the bottom panel, the green trace is the 532 nm optical depth and the red trace is the 1064 nm optical depth. Evidently there is a strong wavelength dependence due to heavy smoke in the PBL. At some points the 532 nm attenuation becomes so great that the optical depth becomes noisy.

Figure 7: Comparison of extinction profiles from CPL, MicroPulse Lidar (MPL) and the Ames Airborne Tracking 14-Channel Sunphotomer (AATS-14) for August 22, 2000. The MPL was sited at Skukuza and the AATS-14 was onboard the CV-580 aircraft. On this day the ER-2 flew within 5 miles of the MPL site, as did the CV-580. Despite slight wavelength differences between the three instruments, there is good agreement in the retrieved extinction profiles. The MPL profile is a 30-minute average, while the CPL profile is a 30-second average.
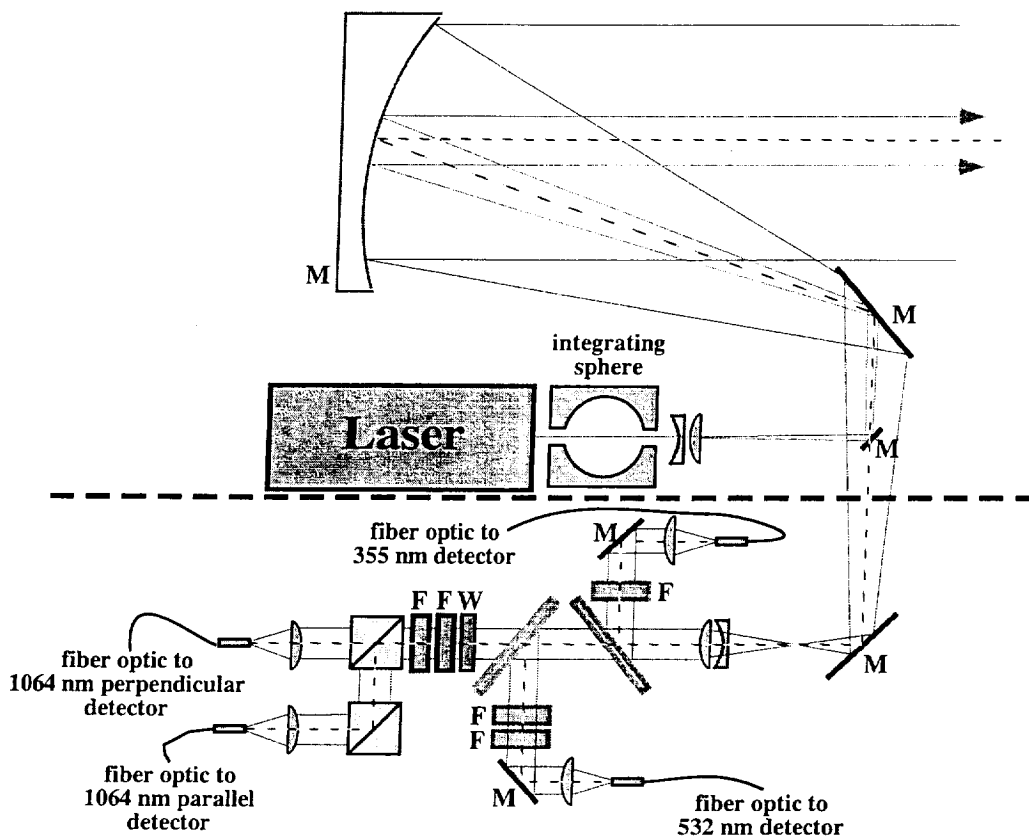
Figure 1: Simplified optical diagram of CPL. Components are labeled as follows: F are interference filters, M are mirrors, and W is a half-wave plate. Components lying above the dashed line are mounted on one side of the optical breadboard, components lying below are mounted on the opposite side.
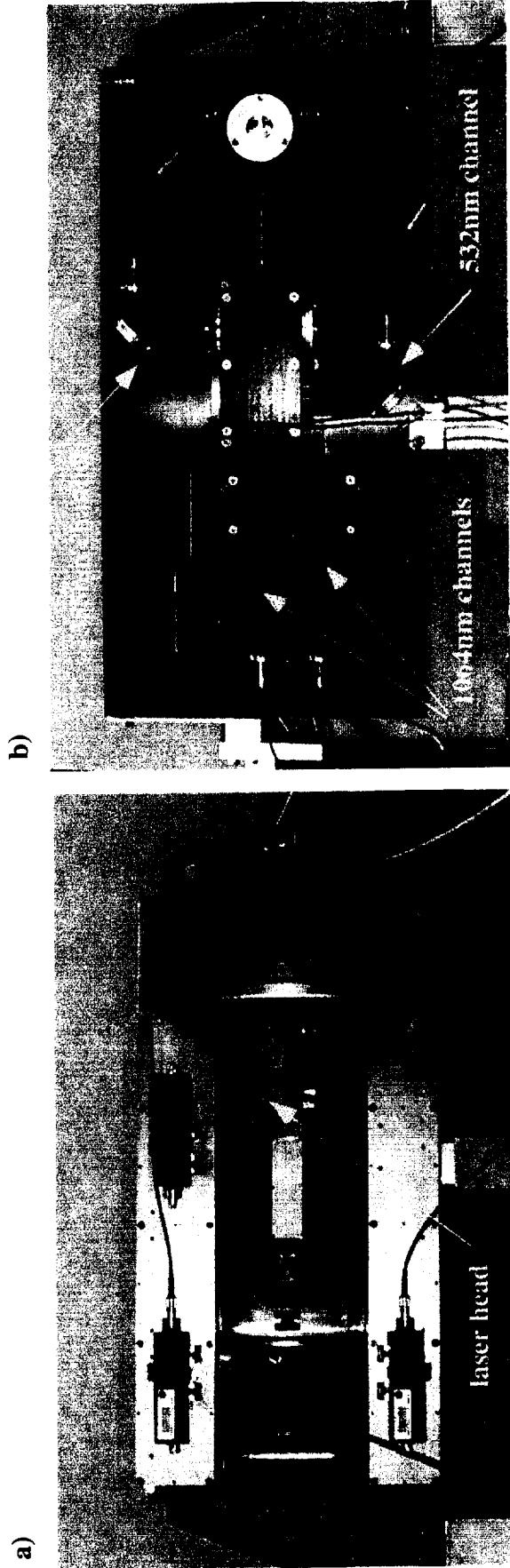
Figure 2: a) Photo of transmitter side of optical breadboard, showing the laser head and off-axis mirror. b) Photo of receiver side of optical breadboard, showing the component layout and the different wavelength channels.

Figure 3: CPL data from September 25, 2000. Top panel shows 1064 nm attenuated backscatter profiles. Middle panel is 532 nm attenuated backscatter profiles. Bottom panel is derived total optical depth. The green trace is the 532 nm optical depth, red trace is 1064 nm. Plot shows the entire flight, illustrating the variability and structure that can be seen in the lidar data. Dense clouds are bright white and cloud shadows are present whenever the lidar signal cannot penetrate through a layer.
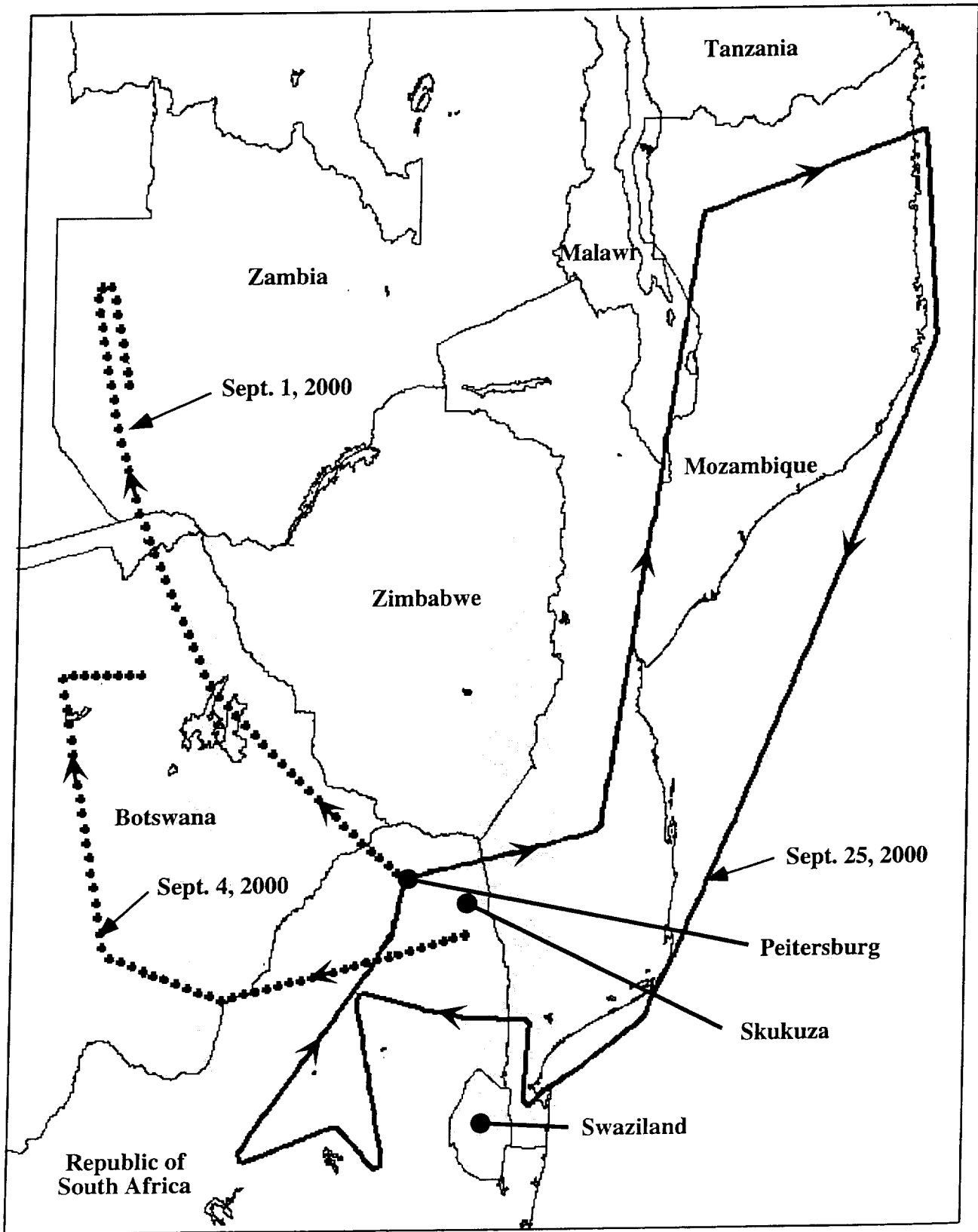
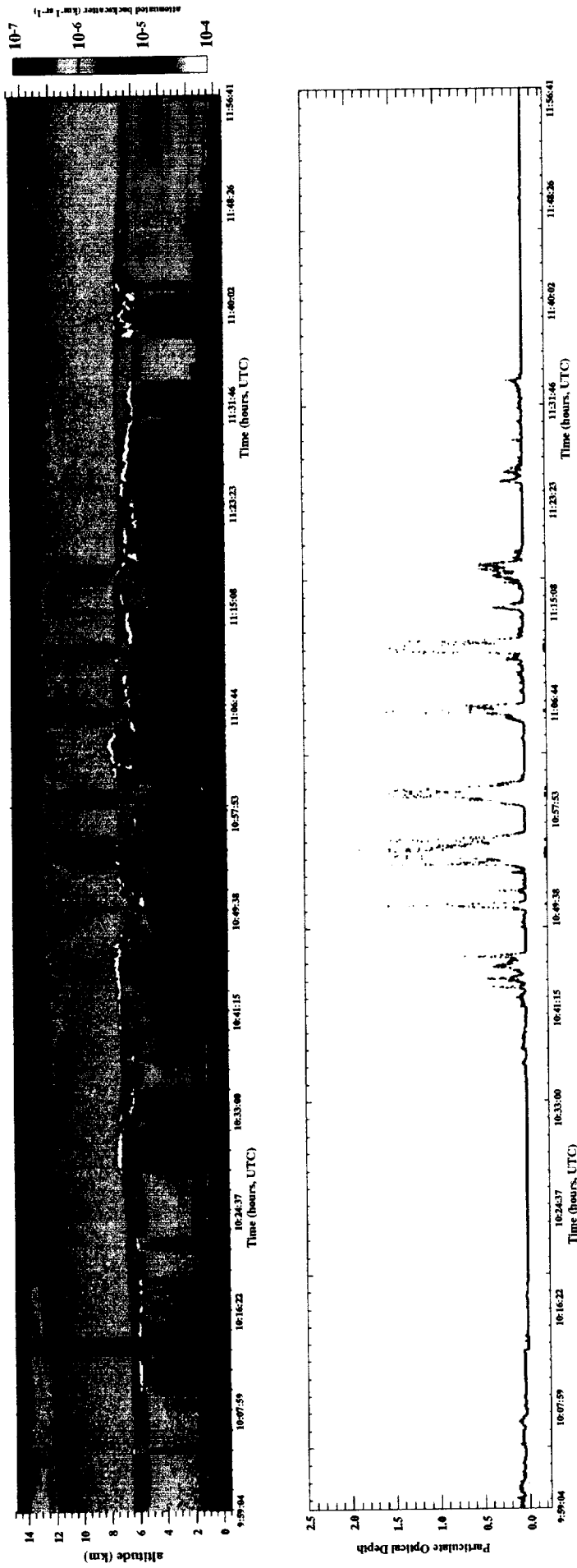**Figure 4**: ER-2 flight tracks for September 1, 4, and 25, 2000.

Figure 5: Cirrus optical depth from September 4, 2000. Plot shows two hours of data. Top panel is the 532 nm attenuated backscatter coefficient, bottom panel is the retrieved cirrus optical depth. The cirrus optical depth is the optical depth due to particulates over the region 9 km to 15 km. In the bottom panel, the green trace is the 532 nm optical depth and the red trace is the 1064 nm optical depth. As expected, there is no wavelength dependence to the cirrus optical depth.
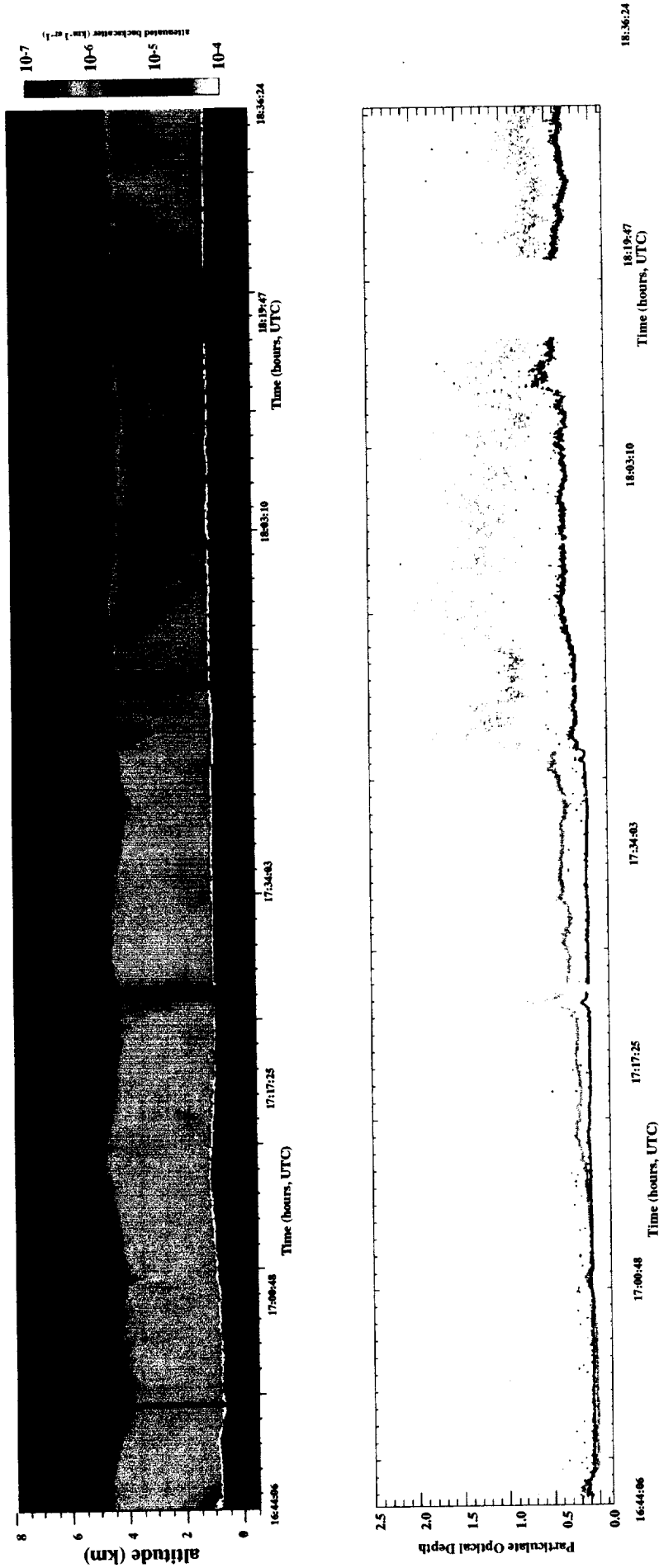
Figure 6: Planetary boundary layer (PBL) optical depth from September 1, 2000. Plot shows two hours of data. Top panel is the 1064 nm attenuated backscatter coefficient, bottom panel is the resultant aerosol optical depth for the PBL only. In the bottom panel, the green trace is the 532 nm optical depth and the red trace is the 1064 nm optical depth. Evidently there is a strong wavelength dependence due to heavy smoke in the PBL. At some points the 532 nm attenuation becomes so great that the optical depth becomes noisy.
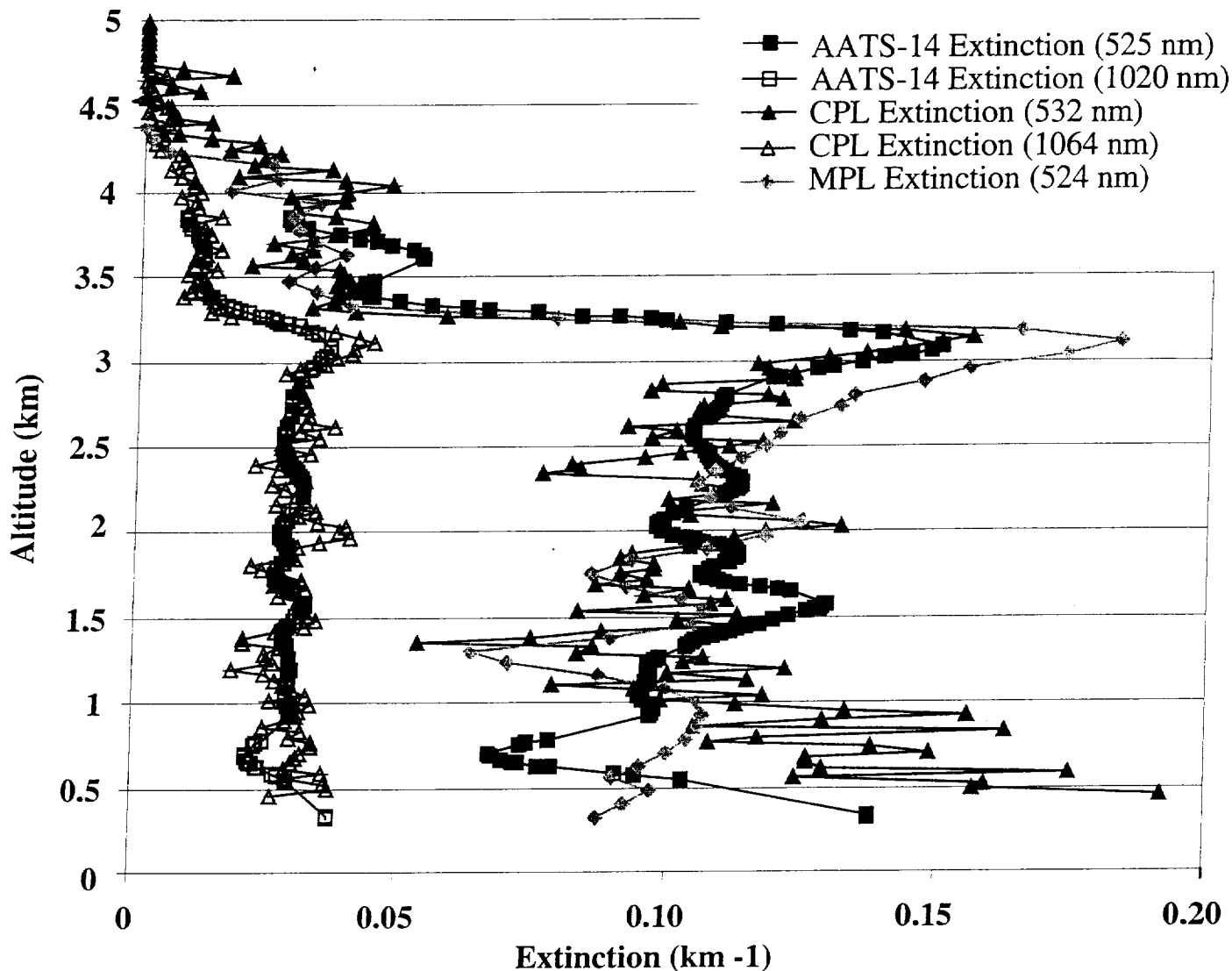
Figure 7: Comparison of extinction profiles from CPL, MicroPulse Lidar (MPL) and the Ames Airborne Tracking 14-Channel Sunphotomer (AATS-14) for August 22, 2000. The MPL was sited at Skukuza and the AATS-14 was onboard the CV-580 aircraft. On this day the ER-2 flew within 5 miles of the MPL site, as did the CV-580. Despite slight wavelength differences between the three instruments, there is good agreement in the retrieved extinction profiles. The MPL profile is a 30-minute average, while the CPL profile is a 30-second average.